PHYSICAL REVIEW B

SOLID STATE

THIRD SERIES, VOL. 5, NO. 2 15 JANUARY 1972

# Temperature-Dependent Electroabsorption on the Indirect Edge of Trigonal Selenium

W. Lingelbach, J. Stuke, and G. Weiser
*Physikalisches Institut der Universität Marburg, Marburg, Germany*

and

J. Treusch*
*Physikalisches Institut der Universität Frankfurt, Frankfurt, Germany*
(Received 6 July 1971)

Electroabsorption was measured on selenium single crystals as a function of temperature, polarization of light, and direction of the modulating electric field. Interpretation along the lines of Elliot's theory of indirect excitonic transitions yields the assignment of the conduction-band minimum to the point $Z=(0,\ 0,\ 1)\pi/c$ of the Brillouin zone or its close neighborhood. The assignment of the maximum of the valence band to the point $H=(\frac{4}{3}\ \pi/a,\ 0,\ \pi/c)$ is reinforced by the reported measurements.

## I. INTRODUCTION

Until recently it has been a matter of some controversy whether the band gap of trigonal selenium is direct or indirect. Some results favored an indirect edge[1,2] whereas other measurements pointed to a direct edge described by the Urbach rule.[3] Band-structure calculations gave rather flat energy bands[4,5] and left the question open, too. Recently Fischer clarified the problem to a great part by absorption measurements on thin crystal platelets grown from the vapor phase.[6] At low temperature several steps were found at the absorption edge for both polarizations of light ($\vec{E}\parallel c$ and $\vec{E}\perp c$) which were interpreted as an indirect excitonic transition with emission of phonons. With increasing temperature these steps disappeared rapidly and also the transition with absorption of phonons could not be observed. Therefore, a determination of the energies of the indirect transition and of the involved phonons was not possible from absorption measurements alone. Fischer derived these values by comparing his electroabsorption results measured at 1.8 °K with the luminescence spectrum of trigonal selenium. Since electroabsorption measurements are particularly useful for an extended analysis of indirect transitions,[7] in the present paper such investigations at different temperatures are reported. Besides the phonon-emission replica of the indirect transition, now the peaks due to absorption of phonons are also observed. Therefore, the energies of the involved phonons can be determined directly and compared with the values given by neutron scattering.[8] The energy of the indirect transition, particularly its temperature dependence, is also obtained and, using results of theoretical band models, the relevant minimum of the conduction band can be located in the Brillouin zone.

## II. EXPERIMENTAL

### A. Experimental Procedure

The measurements were performed on selenium single crystals grown as thin platelets from the vapor phase. The surfaces of these crystals were of good quality so that no further treatment was necessary. This is very advantageous because cleaving and polishing of the samples increase the number of lattice defects in the soft selenium crystals considerably, and thus inhibits the investigation of fine structure in the optical spectra. The thickness of the platelets varied between 15 and 200 $\mu$m. The external electric field was applied using two gold electrodes evaporated on the same crystal face with a distance of 0.5 mm. This arrangement easily allows the orientation of the electric field both parallel and perpendicular to the $c$ axis. The low conductivity of trigonal selenium and the relatively high frequency of the electric field (1 kHz)

exclude anomalous results due to modulation of the temperature within the samples.

The optical system consisted of an iodine-tungsten lamp, a prism double monochromator, polarizer, and photomultiplier, with a spectral resolution of about 1.5 meV. Wavelength, intensity of transmitted light, and its field-induced change were measured simultaneously and automatically evaluated. The lock-in amplifier, detecting the change of transmission, was tuned mostly to the double frequency of the applied sinusoidal electric field because, for trigonal selenium, a quadratic dependence of electroabsorption on field strength exists.[6,9] The response of the electroabsorption at the fundamental frequency is small and differs strongly for the orientation of electric field $\vec{F} \parallel c$ and $\vec{F} \perp c$. This is probably a result of the piezoelectric effect.[10]

The selenium platelets were carefully fixed on electrically insulating but heat-conducting sapphire crystals and clamped to the sample holder of a cryostat having automatic temperature regulation. The temperature could be maintained constant within 1 °K in the range 4.5–200 °K.

### B. Evaluation

No significant influence of the interference of light reflected from both surfaces of the crystals was observed in the experiments. The evaluation of the electroabsorption spectra, therefore, starts from the simple formula for the transmitted intensity $J$,

$$J = J_0(1-R)^2 e^{-\alpha d} , \tag{1}$$

where $J_0$ is the intensity of the incident light, $R$ the reflectivity, $\alpha$ the absorption coefficient, and $d$ the thickness of the sample.

The external electric field induces alterations of both reflectivity and absorption coefficient. The corresponding relative change of the transmitted intensity is

$$-\frac{\Delta J}{J} = \frac{2R}{1-R}\frac{\Delta R}{R} + d\Delta\alpha . \tag{2}$$

From electroreflectance measurements with similar field strength, as used here for electroabsorption, the relative change of the reflectivity $\Delta R/R$ is known to be $10^{-6}$ or less in the investigated spectral range.[10] This effect is negligibly small compared with the value of $\Delta J/J$ which is greater than $10^{-4}$. We obtain, therefore, from (2) the simple expression

$$-\Delta J/J = d\Delta\alpha . \tag{3}$$

According to this formula, thick crystals are favored for electroabsorption measurements because they give a large relative change of transmitted intensity. In the energy region of rapidly increasing absorption coefficient, however, only thin crystals are sufficiently transparent to obtain well-resolved responses. Therefore, the thickness of samples was varied between 15 and 200 $\mu$m.

## III. EXPERIMENTAL RESULTS

### A. Survey of the Electroabsorption Spectrum

The general features of the electroabsorption spectrum and its temperature dependence are shown in Fig. 1 for light polarized parallel to the $c$ axis ($\vec{E} \parallel c$). The upper part gives the spectrum at low temperature which is in good accordance with the results of Fischer[6] measured at 1.8 °K. Above 1.85 eV three strong and two weak maxima are found which correspond to the indirect absorption with emission of five different phonons having the energies quoted above. (The strongest peak near 1.88 eV is reduced by a factor of 10.) Structures which are created by phonon absorption are not yet observed. They arise at higher temperature as can be seen in the spectrum at 38 °K. Here below 1.85 eV an additional peak appears which is assigned to the indirect transition assisted by absorption of the phonon with lowest energy. In this spectrum the phonon emission part of the spectrum above 1.85 eV consists only of the three strong maxima. The small peaks which are well resolved in the upper

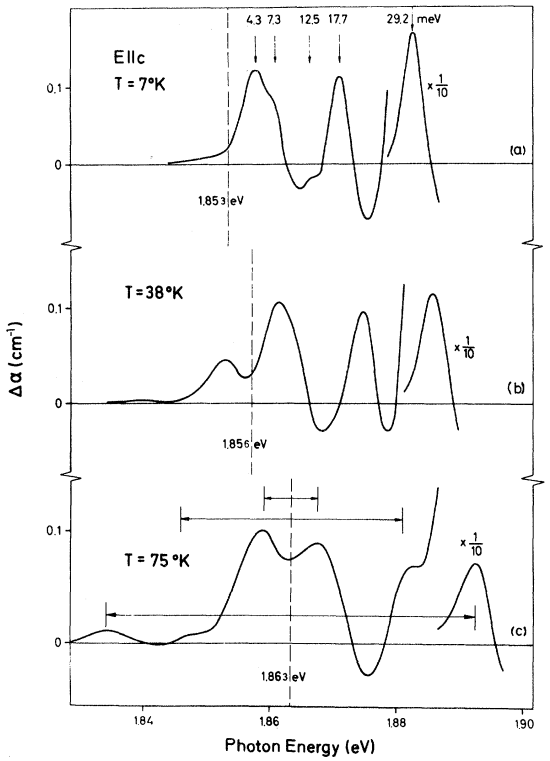


FIG. 1. Electroabsorption spectrum of trigonal selenium for polarization of light $\vec{E} \parallel c$ at different temperatures. Electric field $F = 1.8 \times 10^4$ V/cm perpendicular to $c$ axis. The dashed lines indicate the position of the indirect edge. The marked peaks are reduced by the given factor.

curve are now covered by the strong maxima because these broaden with increasing temperature. Due to this broadening the amplitudes of the peaks decrease, a feature which becomes more evident in the spectrum at 75 °K. In the energy region below 1.85 eV now also the absorption replica of the optical phonons appear since the temperature is high enough to activate these lattice vibrations with higher energy. The six peaks of the spectrum at 75 °K are symmetrical to the dashed line which, therefore, gives the energy of the indirect transition at this temperature. The distance between two corresponding maxima is twice the energy of the phonons involved and the so-determined phonon energies are given above in Fig. 1(a). The energies of the weakly coupling phonons which appear only in the emission part at low temperature are derived from their distance from the dashed line. The 4.3- and 7.3-meV phonons belong to the acoustical branches and the three other phonons with 12.5, 17.7, and 29.2 meV belong to the optical branches of the phonon spectrum of trigonal selenium.[11]

### B. Temperature Dependence of the Electroabsorption Spectrum

The coincidence of the electroabsorption peaks and the steps in the absorption curve reported by Fischer[6] supports strongly the interpretation of the electroabsorption spectrum by an indirect transition. The considerations in this section indicate that this interpretation also explains the temperature dependence of electroabsorption observed in Fig. 1, particularly the different behavior of the phonon-absorption and -emission parts. The magnitude of the phonon-absorption maxima increases with increasing temperature, in contrast to the emission peaks which decrease. This decrease is not uniform for the different emission peaks as is shown in Fig. 2. The amplitude of the maximum corresponding to the optical phonon of 29.2 meV diminishes rapidly whereas the 4.3-meV acoustical-phonon peak decreases much more slowly. At higher temperature the height of the latter maximum even begins to increase slightly.

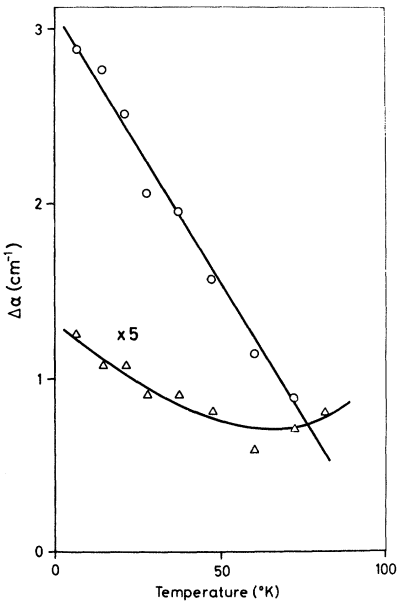


FIG. 2. Temperature dependence of the amplitudes of electroabsorption peaks corresponding to emission of an optical phonon of 29.2 meV (circles) and an acoustical phonon of 4.3 meV (triangles). $F = 1.4 \times 10^4$ V/cm parallel to $c$ axis. The curve for the acoustical phonon is enlarged by a factor of 5.

In the discussion of this temperature dependence we start from the general formula for the absorption coefficient of indirect transitions,

$$\alpha = (n + \tfrac{1}{2} \pm \tfrac{1}{2}) P(\omega, T) , \tag{4}$$

where

$$n = \frac{1}{e^{\hbar\omega_{ph}/kT} - 1} . \tag{5}$$

$P$ gives the transition probability, including the transition density of states, and is nearly the same expression for phonon-absorption and -emission processes. It shall be treated in more detail in the discussion of the band structure in Sec. IV. Besides its dependence on the frequency of light $\omega$, the transition probability depends on temperature due to the lifetime broadening. For the following qualitative considerations it is not relevant whether we observe an exciton or an interband transition.

The Bose factor $n$ giving the phonon population is strongly temperature dependent, rising exponentially at high temperature. The plus sign in Eq. (4) has to be taken for a transition with emission of phonons, the minus sign is valid for a phonon-absorption process.

The external electric field changes only the transition probability and, therefore, leads to the change of the absorption coefficient

$$\Delta\alpha = (n + \tfrac{1}{2} \pm \tfrac{1}{2}) \Delta P(\omega, T) . \tag{6}$$

At low temperature ($kT < \hbar\omega_{ph}$) the Bose factor is small compared with 1. Then the temperature dependence of the phonon-emission peaks [$\Delta\alpha = (n+1) \times \Delta P$] is dominated by the lifetime broadening of the field-induced change of the transition probability $\Delta P$. This broadening by increasing temperature leads to decreasing amplitudes of the field effect[12] and, therefore, to decreasing amplitudes for the phonon-emission peaks. Only at high temperature does the rapidly increasing Bose factor become of influence and may give an increase of the peak amplitudes with temperature in spite of the enhanced broadening. In our experiment this increase is only observed for the peak assigned to the emis-

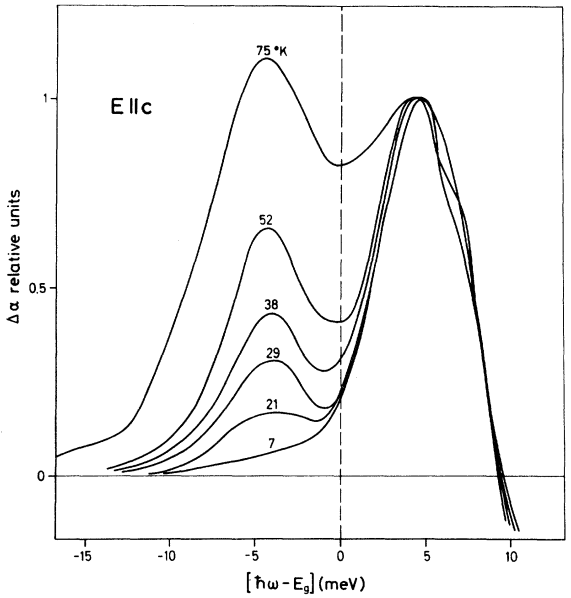


FIG. 3. Temperature dependence of electroabsorption peak corresponding to absorption of the 4.3-meV acoustical phonon in comparison with normalized phonon-emission peak, the temperature shift of the gap being eliminated. $F = 1.8 \times 10^4$ V/cm perpendicular to $c$ axis.

sion of the acoustical phonon with 4.3 meV (Fig. 2) for which $n$ is sufficiently high.

The temperature dependence of the phonon-absorption processes in the electroabsorption spectrum is different from that of the phonon-emission peaks because for phonon absorption the amplitude of the electroabsorption signal is proportional to the Bose factor $n$. The temperature dependence, therefore, is dominated also at low temperatures by this factor, and with increasing temperature the absorption peaks rise according to the strong increase of $n$. Figure 3 demonstrates this rise for the 4.3-meV acoustical phonon in comparison with the corresponding emission maximum. The amplitude of the emission peak is normalized to 1, and the temperature shift of the whole spectrum is eliminated. As expected the amplitude of the phonon-absorption peak increases rapidly above 10 °K. The result that the phonon-absorption peak at 75 °K is higher than the corresponding emission maximum can be explained by the oscillatory character of the structures. They consist obviously of a maximum followed by a negative signal at higher energy, as can be seen from Fig. 1. Since for the 4.3-meV phonon the emission maximum overlaps with the minimum connected with the absorption branch, the emission peak at high temperature becomes lower than the absorption maximum because with increasing height of the absorption peak the depth of the minimum increases also.

For the structures related to optical phonons a similar comparison of the phonon-emission and -absorption peaks was not possible. At low temperature the phonon-absorption replica are very weak and they can only be measured on thick samples. Here, however, the lower transmittance at higher temperature prevents a reliable measurement of the phonon-emission peaks. Absorption and emission of optical phonons, therefore, are observed on the same sample only in a small temperature range, but measurements with different crystals give the same result as for the acoustical phonon. The temperature dependence of the peak which corresponds to the strongly coupling optical phonon of 29.2 meV is shown in Fig. 4. The crystal thickness is about 200 $\mu$m. Similar to the acoustical-phonon–absorption peak in Fig. 3, the response increases rapidly and broadens with rising temperature. The increase starts for this optical phonon at higher temperature because of its larger energy. Below 100 °K the peak shifts with rising temperature significantly to higher energy. Above 100 °K, however, no further shift is observed.

The enhancement of the phonon-absorption peaks with temperature is plotted in Fig. 5 for the acous-

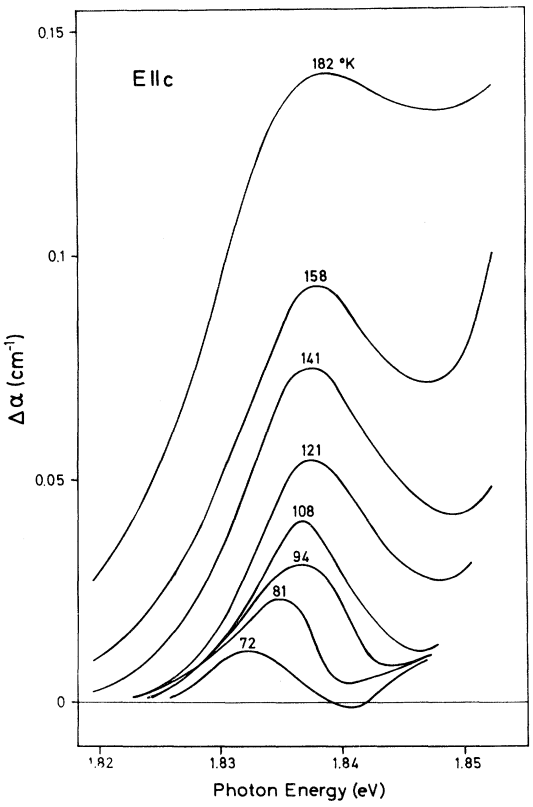


FIG. 4. Temperature dependence of electroabsorption peak corresponding to absorption of an optical phonon of 29.2 meV. $F = 1.4 \times 10^4$ V/cm parallel to $c$ axis.

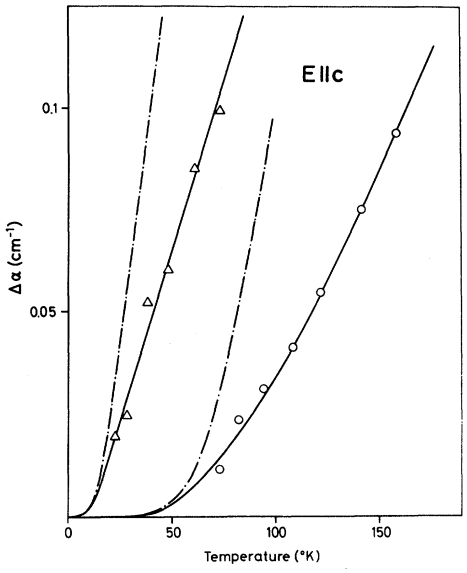


FIG. 5. Temperature dependence of the amplitudes of electroabsorption peaks related to absorption of the optical phonon of 29.2 meV (circles) and the acoustical phonon of 4.3 meV (triangles). The dashed lines represent the corresponding Bose functions. $F = 1.4 \times 10^4$ V/cm perpendicular to $c$ axis.

tical phonon of 4.3 meV and the optical phonon of 29.2 meV. The dashed curves give the corresponding Bose functions fitted to the experimental values at the lowest temperature. The growing deviation of the experimental curves from the Bose functions at high temperature probably is due to the lifetime broadening of the peaks, which is not included here because at high temperature the peaks overlap so that their half-width cannot be resolved. In spite of these deviations the assignment of the electroabsorption spectrum to an indirect transition assisted by several phonons gives a conclusive explanation of the pronounced temperature dependence of the different structures.

### C. Temperature Shift of the Indirect Gap

The sharpness of the peaks of the electroabsorption spectrum allows an accurate determination of the temperature shift of the indirect gap. The result is plotted in Fig. 6. The limit of 180 °K in the data arises because the rapidly increasing electrical conductivity leads at high temperature to uncontrolled heating of the crystal. The upper curve gives for comparison the shift of the direct gap.[10] The energy of the direct transition corresponds to an excitation into an exciton level. The binding energy of this exciton is still unknown; it is estimated to be about 100 meV.[10] According to Fischer[6] the indirect transition also does not go into the conduction band, but creates an exciton, the binding energy of which probably is similar to that of the direct exciton. Both curves, therefore, do not give the energies of the gaps, but rather the transition energies into exciton states. Since the binding energy of excitons, however, depends only slightly on temperature the energy shift of these transitions gives the shift of the band gaps, too.

It is interesting to note that both curves show a similar behavior. Between 30 and 90 °K the indirect, as well as the direct, gap increases linearly with temperature, and above 100 °K they are nearly constant. Since, as shown in the discussion on the band structure, both transitions start from the same valence band but lead to different minima of the conduction band, obviously the temperature shift of the valence band dominates the temperature dependence of both gaps.

The interesting kink in both curves is probably related to the influence of different phonons. The linear part of the temperature shift starts near 20 °K and a comparison with Fig. 5 shows that at this temperature the strong increase of the population of the 4.3-meV phonon sets in. Near 90 °K the shift becomes small and here the Bose factor of the strongly coupling optical phonon rises strongly. We suppose, therefore, that the population of these two phonons causes the kink in the temperature dependence of the energy gaps. Below 90 °K the shift is due to the acoustical phonons which correspond

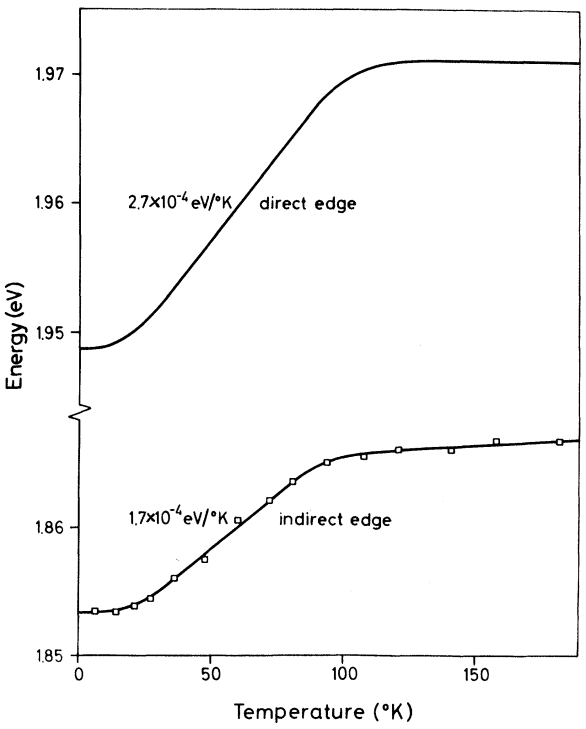


FIG. 6. Temperature shift of the indirect gap of trigonal selenium (lower curve) and of its direct gap (upper curve, taken from Ref. 10).

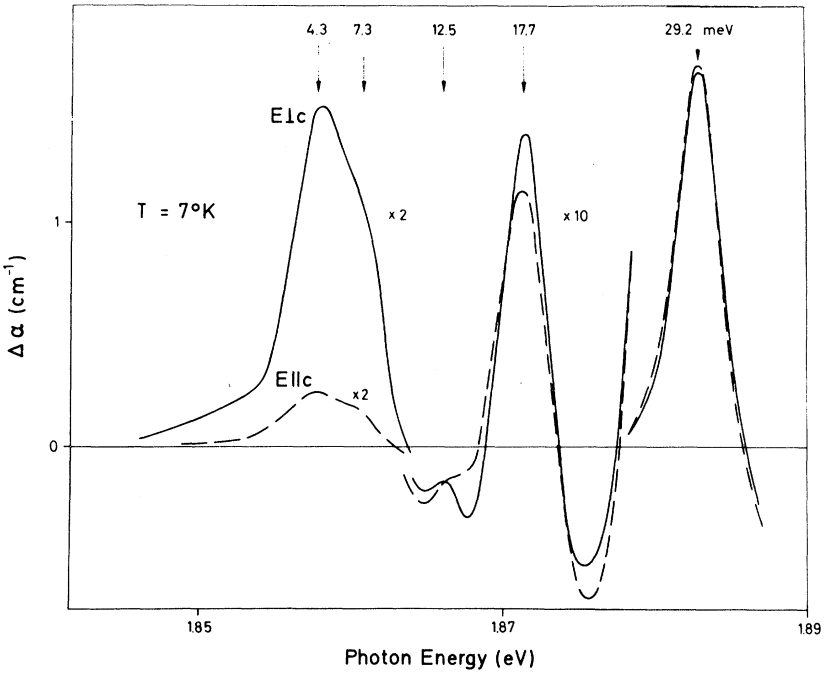


FIG. 7. Electroabsorption spectrum of trigonal selenium for polarization of light perpendicular to the $c$ axis (full curve) in comparison with spectrum for parallel polarization (dashed curve). $F = 1.8 \times 10^4$ V/cm perpendicular to $c$ axis. The marked peaks are enlarged by the given factors.

to the motion of almost rigid chains against one another. Beyond this temperature, however, the influence of the strongly coupling optical phonon dominates, which is due to vibrations of the covalent bonds within the chains.[11] The band gap of the isomorphic tellurium shows a similar behavior,[13] but the influence of the optical phonons dominates here already at lower temperature because of the smaller phonon energy of 18 meV.[8]

### D. Polarization Dependence

All results discussed so far were obtained with light polarized parallel to the $c$ axis. The different rise of the absorption coefficient at the edge for $\vec{E} \perp c$ and $\vec{E} \parallel c$ formerly has been interpreted by different absorption mechanisms.[2] The electroabsorption spectra at 7 °K, however, indicate that no qualitative, but only quantitative, differences for both polarizations exist (Fig. 7). For the peaks assigned to the optical phonons the magnitude of the electroabsorption signal is nearly equal. Both spectra, therefore, correspond to the same indirect transition assisted by the same phonons. The peaks created by the acoustical phonons, however, are for $\vec{E} \perp c$ about 5 to 6 times stronger than for $\vec{E} \parallel c$.

All considerations concerning the temperature dependence of the electroabsorption spectrum with $\vec{E} \parallel c$ are also valid for the spectrum with $\vec{E} \perp c$. The experiments give the same increase of the phonon-absorption peaks, the same broadening and decrease of the phonon-emission maxima, and, finally, also the same temperature shift of the indirect gap is found. The phonon-absorption peak of the acoustical phonon with lowest energy, however, shows an interesting deviation. Different from the measurements with $\vec{E} \parallel c$ (Fig. 3), it appears not symmetrical to the energy of the indirect transition but lies, as shown in Fig. 8, about 1

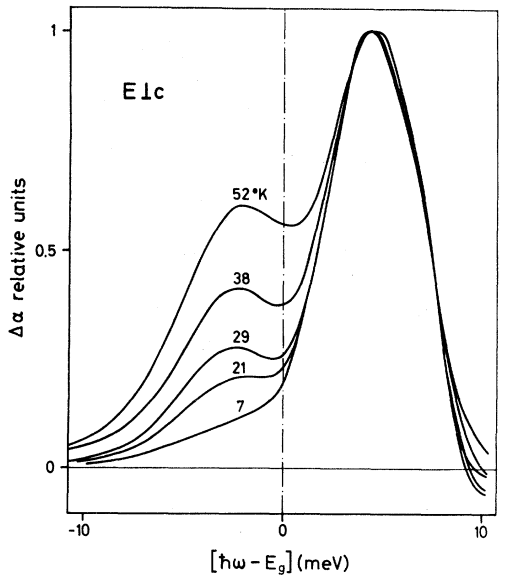


FIG. 8. Temperature dependence of the electroabsorption peak related to absorption of the 4.3-meV acoustical phonon in comparison with the normalized phonon-emission peak for $\vec{E} \perp C$. $F = 1.8 \times 10^4$ V/cm perpendicular to $c$ axis.

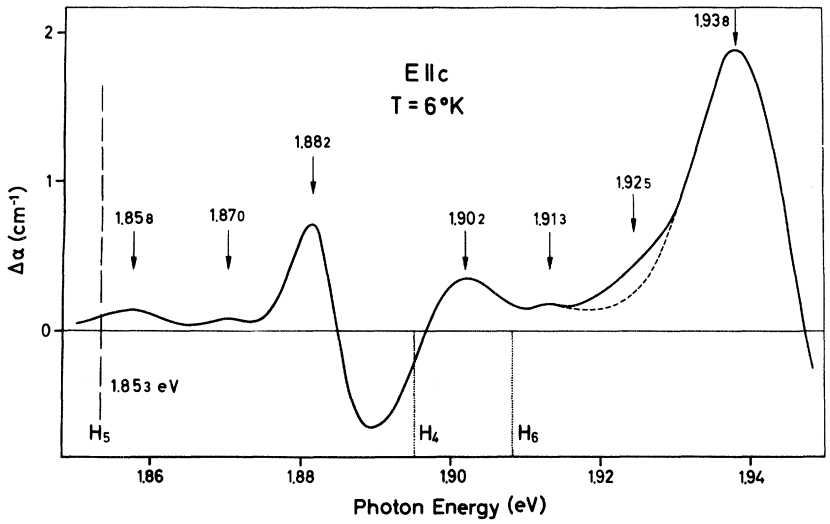


FIG. 9. Electroabsorption spectrum of a thin selenium single crystal ($d \simeq 15$ $\mu$m) at 6 °K. $F = 1.8 \times 10^4$ V/cm parallel to $c$ axis.

meV displaced to higher energy. All other structures, however, are symmetrical and their location, therefore, is independent of the polarization of light. The reason for this remarkable behavior is not yet understood.

### E. Influence of the Field Orientation

The simple electrode configuration used here allowed us to study also the influence of the orientation of the external field $\vec{F}$. For both polarizations of light no difference in the field dependence was observed at any temperature except in the magnitude of the response. A quadratic dependence is found for all peaks in agreement with other measurements.[6,9] However, for the whole spectrum the electroabsorption response is about three times larger for $\vec{F} \parallel c$ than for $\vec{F} \perp c$. The same ratio was found in the electroreflectance response of the first direct transition.[10] From the theory of electroabsorption for interband transitions[14,15] as well as for exciton transitions[15,16] these results indicate an anisotropy of the reduced effective mass with $m_\perp > m_\parallel$. The experimentally found equal anisotropy for the indirect and the first direct transition points to a similar anisotropy of the reduced effective masses for both gaps. Since both transitions start from the same valence-band maximum (Sec. IV) but lead to different conduction-band minima, the anisotropy of the reduced effective masses obviously is dominated by the anisotropy of the mass of the valence band. This means that the effective mass of the holes must be considerably smaller than the effective electron mass, a result which is in agreement with the transport properties of trigonal selenium.[17]

### F. Electroabsorption above 1.89 eV

Above 1.89 eV the absorption coefficient increases rapidly, so that electroabsorption in this region could only be investigated on thin crystals at low temperature. In this energy range further responses are to be expected if the indirect transition starts from the valence-band maximum at point $H$ of the Brillouin zone. Namely, this band is split into three subbands[18] and the transitions from the lower subbands into the conduction band should also take place. Figure 9 shows the electroabsorption spectrum for $\vec{E} \parallel c$ at 6 °K of a crystal with a thickness of about 15 $\mu$m. Because of the low temperature, only the phonon-emission part of the spectrum is found. The structure below 1.89 eV represents the emission spectrum related to the indirect transition at 1.853 eV. (The two weak electroabsorption maxima are lacking here because they can only be observed on thick crystals.) Above 1.89 eV now three further maxima are obtained at 1.902, 1.913, and 1.938 eV. Moreover, near 1.925 eV a response is found. This spectrum seems to be a repetition of the spectrum below 1.89 eV and the question arises whether it can be explained by indirect transitions from the lower valence bands. The first valence band at $H$ splits into three subbands with distances of 42 and 55 meV from the first to the second and the first to the third valence band, respectively.[10] (This is indicated in Fig. 9 by the two vertical dotted lines.) Then the phonon-emission replica of an indirect transition starting from the second $H_4$ band should appear at 1.900, 1.912, and 1.924 eV and the maxima due to the third $H_6$ band analogously at 1.913, 1.925, and 1.937 eV. A comparison of these energy values with the experimental curve in Fig. 9 indicates that indirect transitions from the lower valence bands are probably the reason for these responses. For $\vec{E} \perp c$ the corresponding electroabsorption spectrum could not be measured because the transmitted intensity

for this polarization was too small due to the strong absorption in the tail of the allowed direct exciton transition at 1.948 eV.

A contribution to the large amplitude of the 1.938-eV peak may also be given by the first direct exciton for $\vec{E} \parallel c$. In electroreflection the response of this transition sets in near 1.938 eV for $\vec{E} \perp c$. For $\vec{E} \parallel c$, the polarization used for the results in Fig. 9, this transition is forbidden and no electroreflection signal is observed. However, electroabsorption is much more sensitive than electroreflection[12] and, therefore, a certain contribution of the forbidden direct excitonic transition to the peak at 1.938 eV cannot be excluded.

At high temperature the phonon-absorption replica of the indirect transitions starting from the lower valence bands should also be observed. Most of these replica fall into the emission spectrum related to the transition from the upper $H_5$ band, e.g., the absorption peak which corresponds to the strong phonon-emission maximum at 1.938 eV, a transition from the $H_6$ band, should at 6 °K be located at 1.879 eV. At almost the same energy, namely, at 1.877 eV, an absorption maximum should occur corresponding to the 1.913 eV peak, which is due to the transition starting from the $H_4$ band. With increasing temperature the energy of these absorption replicas is shifted to higher values; their relative location to the neighboring emission peaks at 1.870 and 1.882 eV, however, stays approximately constant. The result shown in Fig. 1, that the minimum between these maxima is considerably lifted with increasing temperature, whereas the depth of the minimum between the 4.3- and 17.7-meV phonon-emission peaks remains almost constant, is probably due to these absorption processes.

## IV. THEORETICAL

To explain the energies, polarization dependences, and relative intensities of the measured phonon replica, we go back to the usual form of the transition probability for indirect transitions as given by Elliott.[19] In second-order perturbation theory one finds for a phonon-assisted transition

$$P \propto \Bigg| \sum_i \frac{\langle a(\vec{k}) | \vec{e} \cdot \vec{p} | i(\vec{k}) \rangle \langle i(\vec{k}) | K_{\mathrm{el,ph}} | e(\vec{k}') \rangle}{E_e(\vec{k}') - E_i(\vec{k}) \pm \hbar\omega_{\mathrm{ph}}} + \sum_j \frac{\langle a(\vec{k}) | K_{\mathrm{el,ph}} | j(\vec{k}') \rangle \langle j(\vec{k}') | \vec{e} \cdot \vec{p} | e(\vec{k}') \rangle}{E_a(\vec{k}) - E_j(\vec{k}') \mp \hbar\omega_{\mathrm{ph}}} \Bigg|^2 \times \delta(E_e(\vec{k}') - E_a(\vec{k}) - \hbar\omega \pm \hbar\omega_{\mathrm{ph}}(\vec{k}' - \vec{k})) \,. \quad (7)$$

Here the first sum corresponds to processes whereby an electron is excited from the top of the valence band to a conduction-band state of the same $k$ value and then is scattered to the final state via phonon creation (upper sign in the denominator) or destruction (lower sign). The sum is to be extended over all possible conduction bands. The second sum corresponds to creation of an electron-hole pair at the $\vec{k}$ vector corresponding to the minimum of the conduction band and scattering of the hole to the final state, i.e., to the top of the valence band. The sum is to be extended over all valence bands that can serve as intermediate states. The phonon population is incorporated into the electron-phonon coupling operator $K_{\mathrm{el,ph}}$ and will not be treated separately here, since the temperature dependence of the replica has been fully discussed in Sec. III A. To obtain more information about $P$ let us proceed as follows: We assume that the conduction-band minimum is located at point $Z = (0, 0, \pi/c)$ of the Brillouin zone, the maximum of the valence band being established at point $H = (\frac{4}{3}\pi/a, 0, \pi/c)$.[10] With this assumption we try to explain the experimental results, and in conclusion we show why this assumption seems to be the only possible one. This procedure is necessary, since up to now neither band structure nor phonon spectrum of trigonal selenium are known to an accuracy that would allow an *a priori* assignment of the indirect gap, the respective phonon branches, and energies. The model band structure shown in Fig. 10 is derived from calculations[4,5,18] and from experimental data concerning direct excitons.[10] It shows that there are two channels (labeled $A$ and $B$) where transitions can take place creating the final-state exciton $H_5$-$Z_6$, which is assumed to be the origin of the phonon replica. From the band model of Sandrock[5] we conclude that the sums over intermediate states can be restricted to the particular states given in Fig. 10, since either the energy denominator would be very large (for the next-higher conduction band in $H$ it would be about 15 times larger than for the lowest one) or the dipole-transition matrix element would

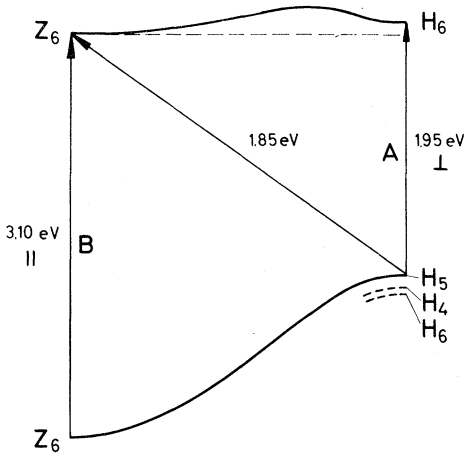


FIG. 10. Model of the indirect gap of trigonal selenium.

be rather small (which reduces the contribution of the second valence band in $Z$ still more than the difference of the corresponding energy denominators does). Optical selection rules now indicate[4] that channel $A$ is allowed only for light polarized perpendicular to the $c$ axis. Channel $B$, however, is allowed for light polarized parallel to the $c$ axis only, since $Z_{6v}$ stems from a single group $Z_1$ representation and $Z_{6c}$ from a $Z_2$ representation, and the selection rules of the spinless case are almost conserved.[10] These optical selection rules are important, since they lead to the conclusion that the first direct transition belonging to the lowest minimum of the conduction band must be allowed for parallel polarization in order to explain the strength of the measured phonon replica for light polarized parallel to the $c$ axis. That excludes point $\Gamma$ = (0, 0, 0) from the further consideration, where the first direct transition is forbidden for parallel polarization. Selection rules for the electron- (hole-) phonon coupling yield the following results[20]:

$$H_5 \times Z_6 = K_3\,, \quad H_6 \times Z_6 = K_1 + K_2 + K_3\,,$$

i.e., the hole can only be scattered by phonons of wave vector $K = (4\pi/3a, 0, 0)$ which transform according to the representation $K_3$ (see Fig. 11). $K_3$ corresponds to the $E$ modes of Chen and Zallen.[22] That may serve as an explanation for the result that the first optical mode $K_2$ (corresponding to $A_2$) at the energy of 12.5 meV is only weakly observed as compared to the $K_3$ mode at 17.7 meV. For the scattering of the electron, however, there is no strict group-theoretical selection rule. Nevertheless, the $K_2$ optical mode is very weak for perpendicular polarization of light, too. The weak coupling of this phonon is probably connected with the rather strange behavior of this "chain twisting" mode. Its macroscopic dipole moment is directed parallel to the $c$ axis and thus perpendicular to the corresponding atomic motions.[22] Moreover, since this dipole moment is caused by interactions between different chains, it might well be small for modes with wave vectors at the edge of the Brillouin zone.

Let us now take actual numbers in order to give an estimate of the relative magnitude of the phonon replica. If the energy of the top of the valence band is set equal to zero, then

$$E_c(Z_6) = 1.835 \text{ eV}, \quad \text{this work}$$

$$E_c(H_6) = 1.95 \text{ eV}\,, \quad \text{Ref. 10}$$

$$E_v(Z_6) = -1.25 \text{ eV}\,, \text{Ref. 10.}$$

These energy values lead to energy denominators of about 100 meV for the transition probability

$$P_\perp \propto \left| \frac{\langle H_{5v} | p_\perp | H_{6c} \rangle \langle H_{6c} | K_{\text{el,ph}} | Z_{6c} \rangle}{E_c(Z_6) - E_c(H_6) \pm \hbar\omega_{\text{ph}}} \right|^2 \delta(\text{energies}) \tag{8}$$

and of about 1.25 eV for

$$P_\parallel \propto \left| \frac{\langle H_{5v} | K_{\text{el,ph}} | Z_{6v} \rangle \langle Z_{6v} | p_\parallel | Z_{6c} \rangle}{E_v(H_5) - E_v(Z_6) \mp \hbar\omega_{\text{ph}}} \right|^2 \delta(\text{energies}). \tag{9}$$

Since optical-dipole matrix elements are independent of whether an acoustical or optical phonon is scattered any variation of the relative strength $P_\perp / P_\parallel$ has to be explained by either the energy denominator or the strength of the phonon coupling.

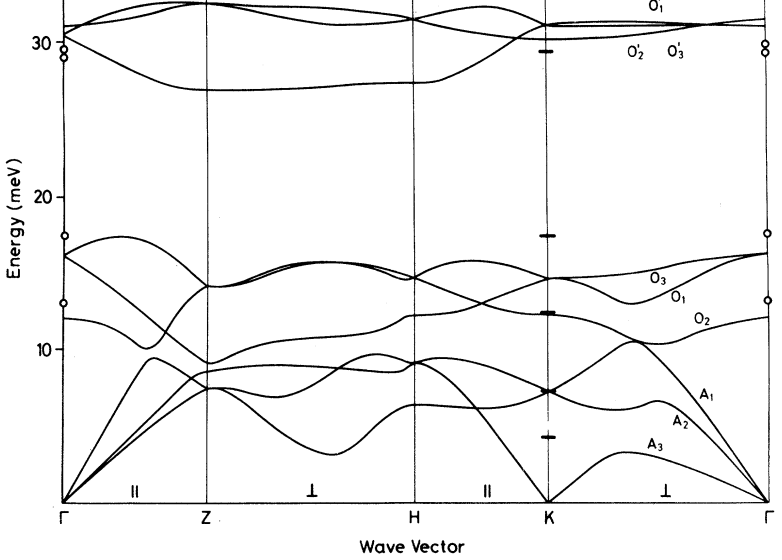


FIG. 11. Calculated phonon spectrum of trigonal selenium (Ref. 11). The bars on the energy scale at point $K$ give the phonon energies found by the electroabsorption measurements; the circles at $\Gamma$ are obtained from infrared reflection and Raman results (Ref. 21). (The vanishing energy of the lowest acoustical-phonon branch at $K$ results from the crude model underlying the calculation in Ref. 11.)

The ratio of the transition probabilities derived from absorption measurements[6] is in good agreement with the ratio of the strength of the differential signals reported here, namely,

$P_\perp/P_\parallel \approx 5$ for the acoustical phonon,

$P_\perp/P_\parallel \approx 1$ for the optical phonons.

From analysis of the energy denominator alone, which is almost constant for $P_\parallel$, and regarding the changes from 90 to 70 meV for $P_\perp$ on going from acoustical to optical phonons, one would expect a trend in the other direction. As a consequence the ratio of the optical-phonon coupling to acoustical-phonon coupling must be larger by a factor of about 8 for coupling with holes than for coupling with electrons, thus favoring channel $B$ for optical-phonon coupling. That seems plausible if one looks at the character of the phonon modes in selenium.[8] Acoustical modes are relative motions of almost rigid chains whereas optical modes strongly affect the covalent bond within a chain by stretching or twisting it. That is just another way of saying that the valence electrons couple strongly to optical phonons, whereas conduction electrons do not.

The structures at energies higher than 1.89 eV, which were treated in Sec. III F, lend themselves, of course, to the same explanation used for the $H_5$-$Z_6$ indirect transition. The only difference is to be seen in the fact that channel $A$ for the transition from the third valence band $H_6$ is also weakly allowed for light polarized parallel to the $c$ axis. As a consequence the structure at 1.938 eV is caused by transitions along channels $B$ *and* $A$ and is therefore particularly strong.

Having established a rather self-consistent explanation of the indirect gap of trigonal selenium as arising from a $H_5$-$Z_6$ transition with an additional $K$ phonon, emitted or absorbed, we now exclude other possibilities. A conduction-band minimum at point $\Gamma$ has already been excluded, since it does not allow transitions involving light polarized parallel to the $c$ axis. Point $K$ can be excluded for purely energetic reasons. All band-structure calculations[4,5] assign to the lowest conduction band at $K$ an energy at least 2 eV above the conduction-band minimum, i.e., a difference far greater than could be attributed to numerical uncertainties. Thus, all of the highly symmetric points are exhausted. If, however, the minimum of the conduction band would lie far away from a symmetry point, then the phonons contributing to the indirect absorption process would also be associated with nonsymmetric points of the Brillouin zone, and the Coulomb interaction splitting of the lower optical $E$ mode should be observed. Moreover, the two acoustical-phonon energies 4.3 and 7.3 meV compare fairly well with neutron spectroscopic data found for polycrystalline selenium samples by Axmann and Gissler.[8] Their values, which represent averages over all van Hove singularities of the phonon spectrum along the edges of the Brillouin zone, are 5.1 and 7.8 meV, respectively. Taking all these exclusive conditions together we come to the conclusion that the minimum of the conduction band indeed is located at point $Z = (0, 0, 1)\ \pi/c$ of the Brillouin zone or in its close neighborhood, where the selection rules still hold approximately and the dispersion of the acoustical-phonon energies is not yet large. As a further interesting result we note that the experimentally determined dispersion of the optical branches, indicated by the circles and bars in Fig. 11, is very small, namely, a few tenths of an meV over the whole axis $\Gamma$-$K$ of the Brillouin zone. The latter result is to be expected from phonon-dispersion calculations,[11] and is a direct consequence of the rather molecular-binding character of trigonal selenium.

---

*Present address: Institut für Physik der Universität Dortmund, Germany.

[1]F. Eckart and W. Henrion, Phys. Status Solidi 2, 841 (1962).

[2]G. G. Roberts, S. Tutihasi, and R. C. Keezer, Phys. Rev. 166, 637 (1968).

[3]W. Henrion, Phys. Status Solidi 12, K113 (1965).

[4]J. Treusch and R. Sandrock, Phys. Status Solidi 16, 487 (1966).

[5]R. Sandrock, Phys. Rev. 169, 642 (1968).

[6]R. Fischer, thesis (University of Frankfurt, 1969) (unpublished); Phys. Rev. (to be published).

[7]A. Frova, P. Handler, F. A. Germano, and D. E. Aspnes, Phys. Rev. 145, A575 (1966).

[8]A. Axmann and W. Gissler, Phys. Status Solidi 19, 721 (1967).

[9]J. Stuke and G. Weiser, Phys. Status Solidi 17, 343 (1966).

[10]G. Weiser and J. Stuke, Phys. Status Solidi 45, 691 (1971).

[11]R. Geick, U. Schröder, and J. Stuke, Phys. Status Solidi 24, 99 (1967).

[12]B. O. Seraphin and N. Bottka, Phys. Rev. 145, 628 (1966).

[13]P. Grosse, *Die Halbleitereigenschaften des Tellur*, Vol. 48 of *Springer Tracts in Modern Physics*, edited by G. Hoehler (Springer, Berlin, 1969).

[14]D. E. Aspnes, Phys. Rev. 153, 972 (1967).

[15]C. M. Penchina, Phys. Rev. 138, A924 (1965).

[16]J. D. Dow and D. Redfield, Phys. Rev. B 1, 3358 (1970).

[17]J. Mort, J. Appl. Phys. 39, 3543 (1968).

[18]B. Kramer and P. Thomas, Phys. Status Solidi 26, 151 (1968).

[19]R. J. Elliott, Phys. Rev. 108, 1384 (1957).

[20]H.-W. Streitwolf, *Gruppentheorie in der Festkörperphysik* (Akademische-Verlagsgesellschaft, Leipzig, 1967).

[21]G. Lucovsky, A. Mooradian, W. Taylor, G. B.

Wright, and R. C. Keezer, Solid State Commun. 5, 113 (1967).

[22]I. Chen and R. Zallen, Phys. Rev. 173, 833 (1968).

PHYSICAL REVIEW B VOLUME 5, NUMBER 2 15 JANUARY 1972

# A Consistency Test for X-Ray Form Factors

A. Marcus Gray
*Watervliet Arsenal, Watervliet, New York* 12180
(Received 11 June 1971)

The validity of electronic band-structure results may be tested by comparing the Fourier transforms of the electronic charge distribution with x-ray structure factors. Measurement of the latter is difficult and liable to relatively large errors. If more than one published set exists it is sometimes difficult to decide which is the most reliable. A simple model for the electronic charge distribution in cubic crystals is proposed, and hence a parametrized expression for x-ray form factors is derived. This is fitted to the available sets of measured form factors by a least-squares technique, giving an indication of the consistency of each set and thus its reliability. Experimental data for Al, diamond, and Si are examined by this method. Electron distributions are drawn in {100} and {110} planes.

## I. INTRODUCTION

A possible method of checking the validity of theoretical band-structure calculations is by comparing the Fourier transforms of the calculated electronic charge distribution with measured x-ray structure factors. However, the derivation of structure factors by experiment is subject to many corrections and the best precision that can presently be obtained is of the order of 1%.[1] Different sets of measurements may show considerable disagreement among each other and it is sometimes difficult to decide which set to use for the comparison with band-structure results.

A simple parametrized theoretical model for the electronic charge distribution in cubic solids is proposed here, and hence a theoretical form-factor expression is derived. The consistency of several sets of measurements is then tested by means of a least-squares fitting procedure.

The approach differs from the conventional use of x-ray diffraction measurements in that the symmetry of the crystal is assumed to be known at the outset.

## II. MODEL CHARGE DISTIRBUTION AND FORM FACTORS

The electron distribution in the crystal $\rho_c(\vec{r})$ can be expressed as

$$\rho_c(\vec{r}) = \sum_{\vec{K}} \hat{\rho}_c(\vec{K})\, e^{-i\vec{K}\cdot\vec{r}} \ , \tag{1}$$

where

$$\hat{\rho}_c(\vec{K}) = \frac{1}{\Omega}\int \rho_c(\vec{r})\, e^{i\vec{K}\cdot\vec{r}}\, d\tau \tag{2}$$

and integration is over the volume of the primitive cell $\Omega$. $\vec{K}$ are reciprocal-lattice vectors. $\rho_c(\vec{r})$ can also be expressed as a superposition of localized charge distributions:

$$\rho_c(\vec{r}) = \sum_{i,j} \rho_s^j(\vec{r} - \vec{\tau}_j - \vec{R}_i), \tag{3}$$

where $\vec{\tau}_j$ fixes the position in the primitive cell, $\vec{R}_i$ is the cell, and where the $\rho_s^j$ are designated as "site distributions." The superscript $j$ distinguishes the different site distributions associated with a primitive cell containing a basis.

Substituting Eq. (3) into Eq. (2) and making the substitutions $\vec{r} - \vec{\tau}_j - \vec{R}_i = \vec{r}'$ results in

$$\hat{\rho}_c(\vec{K}) = \frac{1}{\Omega}\sum_j e^{i\vec{K}\cdot\vec{\tau}_j} \int \rho_s^j(\vec{r}')\, e^{i\vec{K}\cdot\vec{r}'}\, d\tau', \tag{4}$$

where now integration ranges over the extent of the site distribution which may extend beyond the cell boundary. The integral is equivalent to the x-ray form factor[2] $f_j(\vec{K})$ for a charge distirbution $\rho_s^j(\vec{r})$: We have

$$f_j(\vec{K}) = \int \rho_s^j(\vec{r})\, e^{i\vec{K}\cdot\vec{r}}\, d\tau \ , \tag{5}$$

so that

$$\hat{\rho}_c(\vec{K}) = \frac{1}{\Omega}\sum_j e^{i\vec{K}\cdot\vec{\tau}_j} f_j(\vec{K}) \equiv \frac{1}{\Omega}\, F(\vec{K}), \tag{6}$$

where $F(\vec{K})$ is the x-ray structure factor. Equation (6) demonstrates the relation between the Fourier transforms of the crystal charge density and the x-ray structure factors.

It should be noted that x-ray form factors are completely determined from the electron charge distribution and do not depend on the detailed wave-function behavior.

According to Eq. (5), the site charge distribution is the inverse Fourier transform of the form factor.